Towards a safe maximisation of renewable's flexibility in power transmission sub-grids: An MPC approach

Guillaume Ganet–Lepage, Sorin Olaru, Alessio Iovine, Manuel Ruiz, Jean Maeght, Patrick Panciatici

Towards a safe maximisation of renewable's flexibility in power transmission sub-grids: An MPC approach

Guillaume Ganet–Lepage[1], Sorin Olaru[1], Alessio Iovine[1], Manuel Ruiz[2], Jean Maeght[2], Patrick Panciatici[2]

***Abstract*— This paper contributes to the current trend of development of model-based predictive controls for the operation of sub-transmission grids with storage devices and significant distributed generation. As a main contribution of the current work, it is shown that a receding horizon optimization is able to not only automatically handle the curtailment levels but also to indicate the levels of relaxation for the curtailments, whenever they are admissible. The major difficulty in this process resides in the fact that a reduction of the curtailment implies potential increase of the generation power and can lead to transmission line congestions. To avoid the ensuing safety constraint violations, an upper bound is used for the available power to cope with the lack of information when the curtailment is active. The controller's performance is evaluated via simulations through a case study of a real sub-transmission area in the French power grid.**

***Index Terms*— Power transmission network, constrained model predictive control, congestion management**

I. Introduction

In the light of the energy transition of power grids, significant deployment of distributed generation in sub-transmission grids is in full swing. The changing behaviour of the grid, notably as a result of the intermittence of renewable energies, creates several challenges from the monitoring and control points of view. The crucial issues for Transmission System Operators (TSO) is power congestion management, which is an increasingly complex procedure [1], [2]. Poor handling of congestion management carries risks of equipment damage, blackouts, and cascading failures [3]. Within the recent trend in the literature on predictive-control-based design [4]–[6], the works [7]– [8] proposed solutions based on Model-based Predictive Control (MPC) and flexible asset management for congestion management. The controller was shown to optimise the battery usage and the increase in curtailment levels of generators, where curtailment refers to a generation capacity reduction, to balance several objectives: to maintain the line power flows under lines' capacities and to minimize the renewable power curtailed. This paper builds up on these contributions on zonal control management [7]–[9], which is considered nowadays by TSOs as a possible solution for handling power congestion. The contributions here deal with: i) considering the possibility to decrease curtailments ii) whenever the observability of currently available renewable power is lacking, considering a prediction scenario to guarantee the safety of functioning as result of the receding-horizon optimal decision-making.

To promote the first objective, this paper extends the control authority to include decrease of curtailment levels, thus maximising the generation power. The decrease of the curtailment has to cope with the lack of available information on the available power. Notice that, in [8] and [9], the curtailment level is decided with the current available powers measurement and an estimation of the future available powers over a prediction horizon, and the curtailment level is minimized with a penalty in the MPC cost function. Hence, the curtailed power will be reduced if no congestion on the lines is foreseen. However, due to the uncertainty inherent in the available power from renewable energies, the available power can be higher than the generation power, in particular when curtailment is activated.

The existing control methods for the congestion management assume available power and generation power are measurable in real time. This assumption is dropped here: generation power is still measurable but the available power is not. Under some conditions it can be observable, meaning its actual value can be retrieved, but not always, thus, a mechanism is proposed to estimate available power values. This estimation will consider an upper bound along the prediction horizon by including the maximum available power when information on the available power is insufficient to deduce its actual value.

II. Modeling

The definition of a zone is presented now, Fig 1 is an example. A zone is composed of buses (i.e. vertices) and power lines (i.e. edges), see [10]. Within some buses, there is a generator and/or a battery, other buses have no generator nor battery. Zones are connected to the rest of the electrical network (i.e. grid). Consequently, there are two types of lines: the lines within the zone which connect two buses within the zone, and the lines connecting the zone with the rest of the electrical network, which connect one bus within the zone with one bus outside the zone.

[1] Laboratory of Signals and Systems (L2S), CNRS, *CentraleSupélec, Paris-Saclay University*, Gif-sur-Yvette, France {firstname.lastname}@centralesupelec.fr

[2] French Transmission System Operator, *Réseau de Transport d'Électricité (RTE)*, Paris, France {firstname.lastname}@rte-france.com

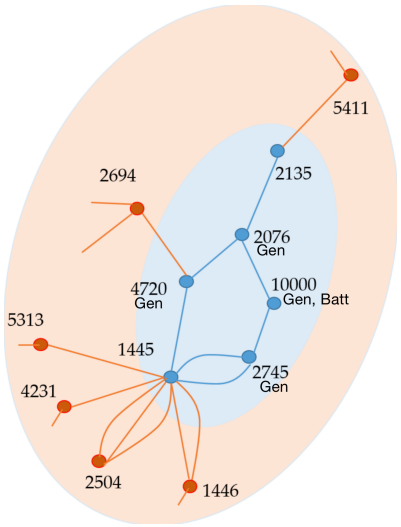

Fig. 1. Zone topology: the zone is in blue, the rest of the electrical network is in orange. For a given bus, the number is the id and the labels *Gen* and *Batt* indicates there is a generator or a battery respectively on the bus.

Precisely, all generators of a zone can have curtailments: a curtailment is not a direct reduction of the generation power but a reduction of the generation capacity. Lastly, the generators are based on renewable energy sources. At any time, the power provided by the renewable energy source that could be used by the generator to generate power is called the available power. In our case, the generators are wind turbines, thus the available power can be visualize as the power provided by the wind that could be used for generation power.

This section recalls the models developed in [7], [10] and [11] for the possibility to use an MPC-based approach that considers partial curtailment for congestion management of a power network zone. The model only considers active powers and no losses in the lines for simplification.

Notations: $\mathcal{Z}^N$ is the set of buses in the considered zone. $\mathcal{Z}^C \subset \mathcal{Z}^N$ is the set of buses with a generator. $\mathcal{Z}^B \subset \mathcal{Z}^N$ is the set of buses with a battery. $\mathcal{Z}^L$ is the set of power lines in the zone. n^N, n^C, n^B, n^L are their cardinalities, respectively. The operator *diag* describes a diagonal matrix composed by the considered elements. The operator *col* produces a single column vector composed by the aggregation of other vectors, while $^\top$ is the transpose operator.

The model: The state variables include the power flow $F_j(t)$ of line $j \in \mathcal{Z}^L$, the battery power output $P^B_m(t)$ and the battery energy $E^B_m(t)$ of battery at bus $m \in \mathcal{Z}^B$; the curtailment power $P^C_n(t)$, the available power $P^A_n(t)$, the generation (i.e. generated) power $P^G_n(t)$, the generation power at the following time $z^G_n(t)$ of generator at bus $n \in \mathcal{Z}^C$ (implicitly equals $P^G_n(t+1)$) . The control inputs are the power variations of $P^C_n(t)$ and $P^B_m(t)$, i.e. $\Delta P^C_n(t)$ and $\Delta P^B_m(t)$. The available power variation $\Delta P^A_n(t)$ represents a disturbance within the zone, while the transit power disturbance $\Delta P^T_l(t)$ describes the unknown power variation at bus l due to power flows transiting between the zone and the rest of the network. The system dynamics of the zone model is defined, $\forall j \in \mathcal{Z}^L$, $\forall n \in \mathcal{Z}^C$, $\forall m \in \mathcal{Z}^B$, $\forall l \in \mathcal{Z}^N$ as:

$$\begin{cases} F_j(t+1) = & F_j(t) + \sum\limits_{m\in\mathcal{Z}^B} b^m_j \Delta P^B_m(t-d) + \\ & \sum\limits_{n\in\mathcal{Z}^C} b^n_j \left[z^G_n(t) - P^G_n(t)\right] + \sum\limits_{l\in\mathcal{Z}^N} b^l_j \Delta P^T_l(t), \\ P^C_n(t+1) = & P^C_n(t) + \Delta P^C_n(t-\tau), \\ P^B_m(t+1) = & P^B_m(t) + \Delta P^B_m(t-d), \\ E^B_m(t+1) = & E^B_m(t) - T c^B_m [P^B_m(t) + \Delta P^B_m(t-d)], \\ P^G_n(t+1) = & z^G_n(t), \\ P^A_n(t+1) = & P^A_n(t) + \Delta P^A_n(t). \end{cases} \tag{1}$$

$$z^G_n(t) = \min\Big(\begin{array}{l} P^A_n(t) + \Delta P^A_n(t), \\ \overline{P}^G_n - P^C_n(t) - \Delta P^C_n(t-\tau) \end{array} \Big) \tag{2}$$

with $b^{m/n/l}_j$ being percentage of power going on line j for a power obtained from bus $m/n/l$ based on the concept of Power Transfer Distribution Factor (PTDF, see [12]), c^B_m is a constant power reduction factor for the batteries, T is the sampling time, d and τ are the time delays of the control actions for the battery power and the generator curtailment, with $\tau \geq d \geq 1$. A generator has a generation capacity $\overline{P}^G_n$, which can be reduced by the power curtailment P^C_n. The remaining capacity is $\overline{P}^G_n - P^C_n(t) - \Delta P^C_n(t-\tau)$. The generation is the minimum between the available power and the remaining capacity.

Equation (2) can be rewritten by introducing the logical variables $\delta^P_n(t) \in \{0,1\}\ \forall\, n \in \mathcal{Z}^C$, which represents what case is the limiting factor for the generation power:

$$\left[\delta^G_n(t) = 1\right] \Leftrightarrow \begin{array}{l} \left[P^A_n(t) + \Delta P^A_n(t)\right. \\ \left. \leq \overline{P}^G_n - P^C_n(t) - \Delta P^C_n(t-\tau)\right]. \end{array}$$

The following system of disjunctive linear inequalities (see [13]) is equivalent to (2):

$$\begin{cases} -\overline{P}^G_n \cdot \delta^G_n(t) & \leq P^A_n(t) + \Delta P^A_n(t) - \overline{P}^G_n + P^C_n(t) \\ & \quad + \Delta P^C_n(t-\tau) \leq \overline{P}^A_n \left(1 - \delta^G_n(t)\right), \\ z^G_n(t) \leq P^A_n & (t) + \Delta P^A_n(t), \\ z^G_n(t) \geq P^A_n & (t) + \Delta P^A_n(t) - \overline{P}^A_n \left(1 - \delta^P_n(t)\right), \\ z^G_n(t) \leq \overline{P}^G_n & - P^C_n(t) - \Delta P^C_n(t-\tau), \\ z^G_n(t) \geq \overline{P}^G_n & \cdot(1 - \delta^P_n(t)) - P^C_n(t) - \Delta P^C_n(t-\tau), \end{cases} \tag{3}$$

where $\overline{P}^A_n$ is the upper bound for the available power. Additionally, the state and control variables respect the

following constraints, $\forall j \in \mathcal{Z}^L$, $\forall n \in \mathcal{Z}^C$, $\forall m \in \mathcal{Z}^B$, $\forall l \in \mathcal{Z}^N$:

$$-\overline{L}_j \leq F_j(t) \leq \overline{L}_j, \quad 0 \leq P_n^C(t) \leq \overline{P}_n^G, \tag{4a}$$

$$\underline{P}_m^B \leq P_m^B(t) \leq \overline{P}_m^B, \tag{4b}$$

$$\underline{E}_m^B \leq E_m^B(t) \leq \overline{E}_m^B, \quad -\overline{P}_n^G \leq \Delta P_n^C(t) \leq \overline{P}_n^G, \tag{4c}$$

$$\underline{P}_m^B - \overline{P}_m^B \leq \Delta P_m^B(t) \leq \overline{P}_m^B - \underline{P}_m^B, \tag{4d}$$

with the upper and lower bounds $\overline{L}_j$, $\overline{P}_n^G > 0$, $\underline{P}_m^B < 0$, $\overline{P}_m^B > 0$, $\underline{E}_m^B > 0$, and $\overline{E}_m^B > 0$. In the following, when necessary, a variable is used without indices, it means the stacked vectors of the variables is used for simplification, e.g. $F(t) = col[F_j(t)]$.

To deal with the known actuator delays, an extended state vector (see [14]) is used. The reformulation consists in storing in the extended state, first the current state, second the queue of controls decided but not yet activated. At each step, the queue of controls shifts: $x(t) = [F(t)\ P^C(t)\ P^B(t)\ E^B(t)\ P^G(t)\ P^A(t)\ \Delta P^C(t-\tau)\ \dots\ \Delta P^C(t-1)\ \Delta P^B(t-d)\ \dots\ \Delta P^B(t-1)]^\top \in \mathbb{R}^{n^L+(3+\tau)n^C+(2+d)n^B}$, $w(t) = [\Delta P^T(t)\ \Delta P^A(t)]^\top \in \mathbb{R}^{n^N+n^C}$, $u(t) = [\Delta P^C(t)\ \Delta P^B(t)]^\top \in \mathbb{R}^{n^C+n^B}$, respectively. Consequently, the resulting undelayed system dynamics derived from (1) and (3) are:

$$\begin{cases} x(t+1) = \tilde{A}x(t) + \tilde{B}u(t) + \tilde{B}_z z^G(t) + \tilde{D}w(t), \\ a^G \geq \tilde{C}_x x(t) + C_z z^G(t) + C_\delta \delta^G(t) + C_w w(t), \end{cases} \tag{5}$$

where the matrices $\tilde{A}$, $\tilde{B}$, $\tilde{B}_z$, $\tilde{D}$, $\tilde{C}_x$, C_z, C_δ, C_w and a^G are suitable matrices. The system model (5) is used for the control design in the next subsection.

III. Control design

In the sequel, the prediction horizon is denoted as N. Moreover, the predicted value of $g(.)$ at the sampling $t+k$ given the available information at the sampling t is denoted as $g(k|t)$.

Hypotheses: In this work, two main hypotheses are different compared to the previous works [7]–[10]. First, curtailment controls $\Delta P_n^C(t)$ can also be negative, while for previous works they were only nonnegative, thus curtailments $P_n^C(t)$ can now increase or decrease. Second, the available power $P_n^A(t)$ is now not measurable. Two cases are possible: in one case, the available power can be calculated exactly; in the other, it is unknown and assumptions are made to estimate it.

Estimations: The estimation procedure predicts two quantities over the prediction horizon: the available power variations $\Delta\widetilde{P_n^A}(k|t)$ within the considered zone, and the transit power disturbance $\Delta\widetilde{P_l^T}(k|t)$. The generation power $P_n^G(t)$ is measured, but not the available power $P_n^A(t)$. The available power $P_n^A(t)$ is known exactly only if the generation power $P_n^G(t)$ is smaller than the remaining capacity $\overline{P}_n^G - P_n^C(t)$, in which case the available power is equal to the generation power. Otherwise, the available power is unknown as greater or equal to the generation power. Based on this rationale, we define the following estimation for the available power $P_n^A(k|t)$, $\forall n \in \mathcal{Z}^C$:

- Case 1: if $P_n^G(t-1) = \overline{P}_n^G - P_n^C(t-1)$ and $P_n^G(t) = \overline{P}_n^G - P_n^C(t)$, then

$$\widetilde{P_n^A}(0|t) = \overline{P}_n^G,\ \Delta\widetilde{P_n^A}(0|t) = 0, \tag{6}$$

- Case 2: otherwise, then

$$\widetilde{P_n^A}(0|t) = P_n^G(t),\ \Delta\widetilde{P_n^A}(0|t) = \overline{\Delta P_n^A}(t), \tag{7}$$

$\overline{\Delta P_n^A}(t)$ is the maximal available power variation at bus n determined from the past historical data until time t. Case 1 corresponds to no information about the available power now and at previous step. Identifying the value of the available power is difficult, thus a worst-case approach for line congestion management is used: the available power is equal to the generation capacity over the whole horizon.

Case 2 corresponds to knowing at the current previous step or both, the available power value. If the available power is known only for the previous step but not now, we consider the available power did not drastically changed in one step, and we estimate the available power is equal to the current generation, which is a lower-bound for the real available power. To mitigate for this estimated available power undervalued compared to reality, the maximal observed available power variation until now $\overline{\Delta P_n^A}(t)$ is applied on the prediction horizon, which results in undervalued available powers at the beginning of the prediction horizon but probably overvalued available powers at its end.

During the prediction horizon, $\Delta\widetilde{P_n^A}(k|t)$ is considered to be constant $\forall\ k \in [0, N-1]$, here k is discrete as representing iterations:

$$\begin{cases} \Delta\widetilde{P_n^A}(k|t) = \Delta\widetilde{P_n^A}(0|t) \\ \widetilde{P_n^A}(k|t) = \max\left(0, \widetilde{P_n^A}(k-1|t) + \Delta\widetilde{P_n^A}(k-1|t)\right) \end{cases} \tag{8}$$

The max operator is to avoid a case of negative predicted available powers, which are meaningless. However, the performance of the transit power disturbance estimation $\Delta\widetilde{P^T}(k|t)$ is out of the scope of this work, thus the simple estimation $\Delta\widetilde{P^T}(k|t) = \mathbf{0}$ is chosen.

MPC design: The *MPC* procedure determines the control signals $u(t)$ using the predicted disturbance sequences $w(k|t)$ and the state feedback $x(t)$ presented in (5). Contrary to [7], this work allows the reverse of decided curtailment for the renewable power generators to maximize benefit of available power if it does not cause power congestion on the transmission lines. Hence, a negative lower bound for the curtailment power variation is applied as described in following constraints for the control signal $u(k|t)$:

$$u_{min} \leq u(k|t) \leq u_{max},\ \forall k \in \{0, \dots, N-1\}, \tag{9a}$$

$$u_{min} = [-\overline{P}^G \quad \underline{P}^B - \overline{P}^B]^\top, \tag{9b}$$

$$u_{max} = [\ \overline{P}^G \quad \overline{P}^B - \underline{P}^B]^\top. \tag{9c}$$

To ensure feasibility of the control problem, soft constraints are imposed to the flow on the power lines $F(k|t)$ for $k \in [d, \tau-1]$ using the softening slack variables $\varepsilon(k|t) \in \mathbb{R}^{n^L}$ such as $\varepsilon(k|t) \geq 0$, $\forall k \in [d, \tau-1]$. The constraints for the state variable $x(k|t)$ are:

- if $d+1 \leq k \leq \tau$,https://tex.stackexchange.com/questions/33969/changing-font-size-of-selected-slides-in-beamer

$$x_{min}(k|t) \leq C_1 x(k|t) \leq x_{max}(k|t), \tag{10a}$$

$$C_1 = \begin{bmatrix} \mathbf{I}_{n^L} & \mathbf{0} & \mathbf{0} & \mathbf{0} & \mathbf{0} \\ \mathbf{0} & \mathbf{0} & \mathbf{I}_{n^B} & \mathbf{0} & \mathbf{0} \\ \mathbf{0} & \mathbf{0} & \mathbf{0} & \mathbf{I}_{n^B} & \mathbf{0} \end{bmatrix}, \tag{10b}$$

$$x_{\min}(k|t) = [-\overline{L}(\mathbf{1}+\varepsilon(k|t)) \quad \underline{P}^B \quad \underline{E}^B]^\top, \tag{10c}$$

$$x_{\max}(k|t) = [\ \overline{L}(\mathbf{1}+\varepsilon(k|t)) \quad \overline{P}^B \quad \overline{E}^B]^\top, \tag{10d}$$

- if $\tau+1 \leq k$,

$$x_{min} \leq C_2 x(k|t) \leq x_{max}, \tag{11a}$$

$$C_2 = [\mathbf{I}_{n^L+2n^C+2n^B} \quad \mathbf{0}], \tag{11b}$$

$$x_{\min}(k|t) = [-\overline{L} \quad \mathbf{0} \quad \underline{P}^B \quad \underline{E}^B \quad \mathbf{0}]^\top, \tag{11c}$$

$$x_{\max}(k|t) = [\ \overline{L} \quad \overline{P}^G \quad \overline{P}^B \quad \overline{E}^B \quad \overline{P}^G]^\top, \tag{11d}$$

A cost function considering actuator delays is defined as:

$$J(t) = \sum_{k=0}^{N-1} \left[\|x(k+1|t) - x_r\|_Q^2 + Ru(k|t) + \|\varepsilon(k|t)\|_\beta^2 \right] \tag{12}$$

where $x_r = [\mathbf{0}_{n^L+2*n^C+(\tau+1)n^C+(d+2)n^B \times 1}]$ is the state reference [7], meaning ideally no curtailment is desired nor the battery usage. Q is a positive semi-definite matrix (whose zero values on the diagonal are considered for variables lacking references, e.g., F or P^A), $R \in \mathbb{R}_+^{n^C+n^B}$ gathers positive elements, and β is a positive scalar. Since one of the goals is to reduce P_n^C, a weight different from zero is considered on the elements of Q multiplying P_n^C. We remark that the linear term of the cost function with respect to the control input u contributes to favour the curtailment to decrease. Thus, the MPC optimisation problem is defined as the following Mixed-Integer Quadratic Program (MIQP, see [15]):

$$\begin{aligned} \mathcal{O}_0 = & \underset{\{u(0|t),\ldots,u(N-1|t)\}}{\operatorname{argmin}} \quad J(t) \text{ in (12)} \\ s.t.\ & (5)\ \forall k \in [0, N-1],\ (9)\ \forall k \in [0, N-1], \\ & (10)\ \forall k \in [d+1, \tau],\ (11)\ \forall k \in [\tau+1, N]. \end{aligned} \tag{13}$$

Once the optimization problem is solved, the first control $u(0|t)$ is decided, the curtailment control $\Delta P^C(0|t)$ will be applied at instant $t+\tau$ and the battery control $\Delta P^B(0|t)$ at $t+d$ due to the respective delays, to determine the curtailment power at instant $t+\tau+1$ and the battery power output at $t+d+1$, respectively. Consequently, for the simulation in the following section, we decide the prediction horizon N to be equal to the longest control delay (the curtailment control) plus one iteration such that the resulting state obtained from this control is evaluated in the prediction horizon of the MPC, thus $N = \tau+1$.

TABLE I

System, control and simulation parameters.

Parameter	Value
Number of buses n^N and of lines n^L	6 and 7
Number of curtailed generators n^C	4
Number of batteries n^B	1
Line power limit $\overline{L_j}$ [MW]	45
Generator power limits $\overline{P}^G$ [MW]	$[66\ 54\ 10\ 78]^\top$
Available power limits $\overline{P}^A$ [MW]	$[66\ 54\ 10\ 78]^\top$
Battery power limits $[\underline{P}^B\ \overline{P}^B]$ [MW]	[-10 10]
Battery delay d [s]	5
Curtailment actuator delay τ [s]	45
Prediction horizon N	10
State weight matrix Q	$diag\{\mathbf{0}_{7\times7} \quad 10^3\mathbf{I}_4 \quad \mathbf{0}_{39\times39}\}$
Input weight matrix R	$[\mathbf{1}_{1\times4} \quad 0]$
State reference x_r	$[\mathbf{0}_{50\times1}]$
Relaxation weight β	10^7
Sampling time T [s]	5
Simulation time [s]	1200

IV. Simulation results

This section presents closed-loop simulations of the sub-transmission grid (i.e. a zone) depicted in Fig. 1. The zone is composed of six buses, seven lines, four generators and one battery. The available power profiles are based on real data (see [10]). The management of the battery energy capacity is not a focus in this simulation, thus the associated constraint is removed, as if the battery was of infinite size, but the battery power capacity constraint remains. The parameters of the model, control problem, and simulations are presented in Table I. The simulations are implemented in MATLAB 2022a, with the open toolbox MATPOWER [16]. The predictive control formulations are described and solved using YALMIP [17]. The small size of the problem allows each MIQP to be solved in less than a second, which is largely lower than the sampling time of five seconds.

We introduce the figures of the simulation results: Fig. 2 shows generation powers, available powers and remaining capacity of the four generators in the zone. Fig. 3 shows two line power flows: the two lines with the highest overflows in open-loop conditions, i.e. when the zone has no controller, and they are responsible for almost all control actions. Fig. 4 shows the battery power outputs on bus 10000, its variation is the battery controls.

First, the case of open-loop conditions is considered: visible on Fig. 2 with the black curves, the generation powers of all generators start low. They highly increase until 400 or 500 seconds depending on the generator. Then, the generation powers roughly stagnate for 300 seconds, followed by generation powers reaching the generators' capacity, then for some generators, the generation decreases. The consequence on the line power flows are visible on Fig. 3 in black: the power flows are low until 400 seconds, which is the moment when they are close to the

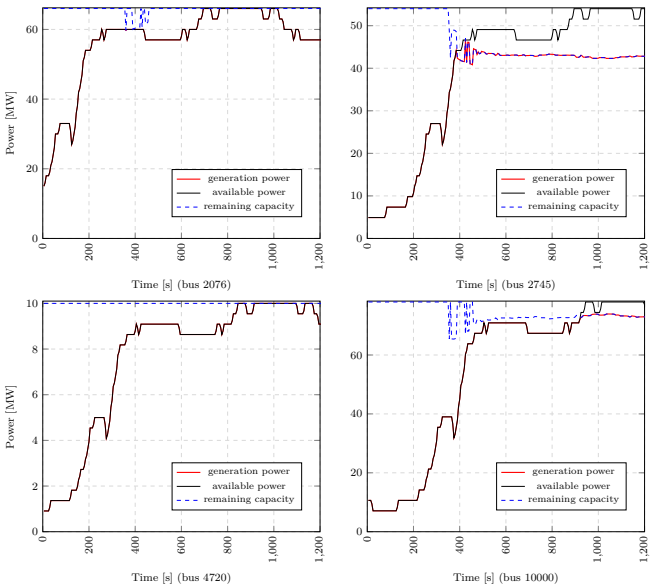

Fig. 2. From top-left to bottom-right, row-wise, generators at bus 2076, 2745, 4720, 10000: generation power P_n^G, available power P_n^A and remaining capacity $\overline{P}_n^G - P_n^C$.

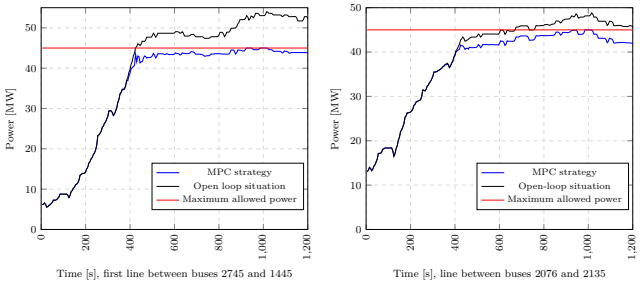

Fig. 3. Line Power flows Fj: a comparison between the open-loop situation versus the closed-loop via MPC. On the right, the first line between buses 2745 and 1445, on the left is the line buses 2076 and 2135.

maximum allowed power, i.e. the limit. The line between buses 2745 and 1445 exceeds the limit from 400 seconds until the end of the simulation, with a high overflow after 900 seconds. The power flow on line between buses 2076 and 2135 slowly increase from 400 to 1000 seconds, the open-loop overflows start at 600 seconds until the end of the simulation.

Second, the case of simulation with MPC is considered: To tackle the overflows that appears on the lines of Fig. 3, the MPC takes control actions both on the battery and the generators. In the first 400 seconds, no overflow are expected so the battery control lever is not activated as long as the congestion episode is not active. After 400 seconds, the production trends are predicting long standing violations of the line constraints between buses 2745 and 1445 (cf. Fig. 3), thus battery controls are triggered (cf. Fig. 4), then the battery power output is practically at its maximum capacity (in negative value) to help with line power flow reduction. Towards the end of the congestion episode, the flows decrease, thus the

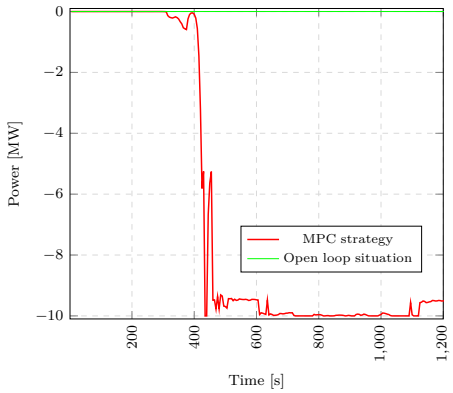

Fig. 4. Battery power output P^B of the battery at bus 10000.

gap to reach an overflow increases; as the battery power output reference is 0, then the battery power gradually decreases. Regarding the generators, cf. Fig. 2, generators on buses 2745 and 10000 are curtailed after 400 seconds to avoid line overflows. The MPC decides to curtail mostly on these two generators as they are the most influential for the two lines of Fig. 3 due to the topology through their respective PTDF coefficients. As long as the available power does not meet the capacity constraints, the generation power coincides with the available one, typically until 400 seconds for the generator on bus 2745 on Fig. 2. For the generator on bus 2745, after 400 seconds, the generation power is limited by the remaining capacity decided by the MPC, thus the former is equal to the later. Consequently, despite the very high available power from 800 seconds to 1100 seconds, the generation power is unaffected. Thanks to the MPC's curtailment and battery controls, the line power flows of Fig. 3 remains under the maximum allowed power, thus fulfilling the overall objectives.

Third, with respect to the main contribution of our work, let us present a situation well-managed thanks to negative curtailment controls despite the lack of measurement of the available power. Recall that the MPC decides controls by predicting on a 50-second receding horizon due to the curtailment delay of 45 seconds. The predictive behavior of the control strategy becomes apparent after 310 seconds of simulation. Indeed the available power variations around 310 seconds are steep on all generators, see Fig. 2, thus the controller predicts that the power flows will come against the line limitations in the prediction horizon based on the trends in the available powers. Consequently, curtailment controls are decided on generators on buses 2076, 2745 and 10000, which are activated 45 seconds later leading to remaining capacity reductions (blue dotted curves on Fig. 2). However, as time goes by, the MPC is aware that the generation powers are not too high for the power lines and cancels out power curtailments with negative curtailment controls. Notably, the time-varying generation capacity on bus 2076 (Fig. 2) is brought back to the initial and maximum capacity at

450 seconds and until the end, and the generation power is maximum afterwards. If only nonnegative curtailment controls were allowed, the generation power from 700 to 1100 seconds on this generator would not have been equal to the available power due to curtailments, resulting in loss of renewable generations. Additionally, at the end of the simulation, the stabilized remaining capacities of generators at buses 2076, 2745 and 10000 are higher than their values around 400 seconds, so the MPC allows for a greater renewable generation power than if only nonnegative curtailment controls were allowed. Regarding the fact that available powers are not measurable, the conservative hypothesis explained in previous sections result in line power flows not exceeding the limit during this simulation, even though the limit is a soft constraint which could be temporary violated.

The most important feature of the methodology presented in this paper is the capability of reversing a curtailment decision. This provides an important flexibility and a maximization of the renewable energy injection but has to be done on safety grounds, i.e. with respect to the line power flow limitations. In Figures 2, the remaining capacity follows a non-monotonic profile. This shows that a curtailment action can be reversible, which is a step forward with respect to the state of the art. The decision for its relaxation is done by integrating the safety constraints. As such the limitations are monitored in real-time and the impact on the generation power is minimized.

The decisions related to the curtailment activation or relaxation are clarified by the trajectories of the power flows on the line which represent the state variables in the proposed dynamical model. In Figures 3, the control is maintaining the power flow below the power line limit which represents the sensitive limitation from which an automatic safety policy would be activated. It is clear that despite the congestion episode, the trajectories are driven on a safe profile, in a zone which takes the full advantage of the available capacity all by avoiding the violation of the constraints which is inevitable in the absence of an active control (black curves). The power line limit is a soft constraint: technically, the line power flows can exceed the limit for a short amount of time, but here there is no overflow because of the safeguards made regarding the available power evolution estimation for the MPC.

V. Conclusions and prospects

This work presented a predictive control strategy for congestion management in sub-transmission power grids with high levels of renewable-energy-based generation. In this paper, the controller's curtailment actions are extended to being able to lift previously-imposed curtailment levels. The major difficulty is related to the uncertainty related to the power available once the curtailment lever is active. The controller's performance is analysed with respect to various objectives e.g. optimisation of economic cost, operational safety, etc.

Future steps currently underway include the comparison of the controller performance based on a linearized model in order to decrease the complexity of the implementation. Another important research subject is the inclusion of logical constraints that avoid curtailment relaxations consecutive to a curtailment activation.

References

[1] B. Meyer, J. Astic, P. Meyer, F. Sardou, C. Poumarede, N. Couturier, M. Fontaine, C. Lemaitre, J. Maeght, and C. Straub, "Power Transmission Technologies and Solutions: The Latest Advances at RTE, the French Transmission System Operator," *IEEE Power and Energy Magazine*, vol. 18, no. 2, pp. 43–52, 2020.

[2] L. Che, X. Liu, and Z. Shuai, "Optimal transmission overloads mitigation following disturbances in power systems," *IEEE Transactions on Industrial Informatics*, vol. 15, no. 5, pp. 2592 – 2604, 2019.

[3] F. Monforti-Ferrario and M. P. Blanco, "The impact of power network congestion, its consequences and mitigation measures on air pollutants and greenhouse gases emissions. A case from Germany," *Renewable and Sustainable Energy Reviews*, vol. 150, p. 111501, 2021.

[4] M. R. Almassalkhi and I. A. Hiskens, "Model-Predictive Cascade Mitigation in Electric Power Systems With Storage and Renewables; Part I: Theory and Implementation," *IEEE Transactions on Power Systems*, vol. 30, no. 1, pp. 67–77, Jan 2015.

[5] ——, "Model-Predictive Cascade Mitigation in Electric Power Systems With Storage and Renewables; Part II: Case-Study," *IEEE Transactions on Power Systems*, vol. 30, no. 1, pp. 78–87, Jan 2015.

[6] M. Mehrabankhomartash, M. Saeedifard, and S. Grijalva, "Model predictive control based ac line overload alleviation by using multi-terminal dc grids," *IEEE Transactions on Power Systems*, vol. 35, no. 1, pp. 177–187, 2020.

[7] D.-T. Hoang, S. Olaru, A. Iovine, J. Maeght, P. Panciatici, and M. Ruiz, "Power Congestion Management of a sub-Transmission Area Power Network using Partial Renewable Power Curtailment via MPC," in *60th IEEE Conference on Decision and Control*, 2021, pp. 6351–6358.

[8] T.-H. Pham, A. Iovine, S. Olaru, J. Maeght, P. Panciatici, and M. Ruiz, "Advanced management of network overload in areas with Renewable Energies Sources," in *11th IFAC Symposium on Control of Power and Energy Systems (CPES)*, 2022.

[9] N. Dkhili, A. Iovine, S. Olaru, J. Maeght, P. Panciatici, and M. Ruiz, "Predictive control based on stochastic disturbance trajectories for congestion management in sub-transmission grids," in *18th IFAC Workshop on Control Applications of Optimization (CAO)*, 2022.

[10] A. Iovine, D.-T. Hoang, S. Olaru, J. Maeght, P. Panciatici, and M. Ruiz, "Modeling the partial renewable power curtailment for transmission network management," in *2021 IEEE Madrid PowerTech*, 2021, pp. 1–6.

[11] T.-H. Pham, A. Iovine, S. Olaru, J. Maeght, P. Panciatici, and M. Ruiz, "Nonlinearity handling in MPC for Power Congestion management in sub-transmission areas," in *18th IFAC Workshop on Control Applications of Optimization (CAO)*, 2022.

[12] X. Cheng and T. Overbye, "PTDF-based power system equivalents," *IEEE Transactions on Power Systems*, vol. 20, no. 4, pp. 1868–1876, 2005.

[13] E. Balas, "Disjunctive Programming," in *Discrete Optimization II*, ser. Annals of Discrete Mathematics. Elsevier, 1979, vol. 5, pp. 3–51, iSSN: 0167-5060.

[14] E. Fridman, *Introduction to Time-Delay Systems Analysis and Control*. Springer, 2014.

[15] R. Lazimy, "Mixed-integer quadratic programming," *Mathematical Programming*, vol. 22, no. 1, pp. 332–349, Dec. 1982.

[16] R. D. Zimmerman, C. E. Murillo-Sánchez, and R. J. Thomas, "Matpower: Steady-state operations, planning, and analysis tools for power systems research and education," *IEEE Transactions on Power Systems*, vol. 26, no. 1, pp. 12–19, 2011.

[17] J. Löfberg, "Yalmip : A toolbox for modeling and optimization in matlab," in *In Proceedings of the CACSD Conference*, Taipei, Taiwan, 2004.